Violet Grove time-lapse data revisited: a surface-consistent matching filters application

Mahdi Almutlaq and Gary F. Margrave

ABSTRACT

We apply the surface-consistent matching filters to a real data set from the Violet Grove area in central Alberta. Detecting time-lapse difference on this data has proved to be difficult due the small impedance contrast at the Cardium reservoir where CO_2 is injected. However, we decided to examine the matching filters algorithm on this data for two main reasons: 1) to test the algorithm on a real data set and 2) to compare our results with previous processing on the same data. For this purpose, we evaluate two zones: a shallow one above the reservoir centered on the Ardley Coal Zone, and a deeper one below the reservoir.

After applying the surface-consistent matching filters to the monitor survey, we reduce most of the mismatch caused by acquisition differences and near surface variations. Differences caused by nonrepeatable noise in the data are difficult to remove since they are nonstationary. The shallow window above the reservoir is dominated by the near-surface noise compared to the deeper window of analysis. Despite this issue, we notice an improvement in the pre-stack and the post-stack image after applying the surface-consistent matching filters.

INTRODUCTION

CO_2 sequestration, also known as carbon capture and storage (CCS) in deep geological formations, is a multidisciplinary technology that involves capturing, transporting, and storing CO_2 gas. The Sleipner field in Norway is one of the large scale industrial CCS projects that proved successful and many authors have published data from this field including Zweigel et al. (2001), Arts et al. (2002), and Chadwick et al. (2009). Several similar CCS projects were implemented in different places around the world and the Weyburn field in Canada for enhanced oil recovery (EOR) is another example with many published work including Brown et al. (2002), Terrell et al. (2002), Davis et al. (2003), Li (2003), and White (2009). These two projects, even though each has a different goal, are considered by industry the standard on how seismic can be part of the CCS technology and the Sleipner field seismic monitoring of the injected CO_2 sets a good example.

The earth's subsurface experience some effects due to gas injection. These effects include, but not limited to, P-wave and S-wave speeds decrease (Wang et al., 1998; Mavko and Mukerji, 1998; Wang, 2001), density decrease (Avseth et al., 2005), increase in seismic wave attenuation (Hilterman, 2001), and anisotropy (MacBeth and Lynn, 2000).

Surface-consistent matching filters (Almutlaq and Margrave, 2010) is an algorithm based on two well known concepts: the surface-consistent hypothethesis and the matching filter. We explained how the algorithm works on a time-lapse model data (Almutlaq and Margrave, 2012a). The objective of this paper is to apply the algorithm to a time-lapse data set from Violet Grove and compare the results to the previous processing.

Area of study

The Pembina Oil Field is about 100 km southwest of Edmonton, in central Alberta (Figure 1). This is the most aerially extensive oil field in the world covering approximately 4000 km^2 (Dashtgard et al., 2006) with huge oil and gas reserves. Discovered in 1953, production in this field is from Devonian to Tertiary strata with the Upper Cretaceous Cardium Formation being the most prolific (Dashtgard et al., 2006).

The site of CO_2 sequestration is known as Violet Grove near the center of the Pembina Field and injection of CO_2 is in the Upper Cretaceous Cardium Formation in the period between March 2005 and March 2007 (Alshuhail et al., 2011). According to Hitchon (2009), this Formation has been subdivided into the lower dominantly arenaceous Pembina River Member and the upper dominantly argilaceous Cardium Zone Member. The Pembina River Member is a coarsening-upward sequence, dominated by shale layers at the base and sandstone layers at the top, and is capped by chert conglomerate. The Cardium Formation overlies the Blackstone Formation which is dominated by black shale, and is overlain by shales of the Wapiabi Formation (Figure 2).

At this site, the Cardium Formation consists of three distinct sandstone units (upper, middle and lower) separated by two shale units (Figure 2). The maximum cumulative thickness of the reservoir units is about 20 m at a depth of about 1600 m in the northeast to about 1650 m in the southwest of the pilot study area. Table 1 summarized some of the physical properties of the Cardium Formation in Violet Grove area.

Table 1: Physical properties of the Cardium Formation from the study area (Hitchon, 2009).

Lithology	Ave. porosity (%)	Ave. K (mD)	Temp. (C^o)	Pressure (MPa)
Conglomerate	8	31	50	19
Upper and middle sand	16	21	50	19
Lower sand	-	10.5	50	19

TIME-LAPSE DATA: ACQUISITION AND PREVIOUS PROCESSING

Three phases of surface and borehole seismic data were acquired at the Pembina Cardium CO_2-EOR pilot site between March 2005 and March 2007. During this period, approximately 60,000 tonnes of CO_2 were injected in the Cardium Reservoir. A time-lapse seismic data set was designed and acquired as part of the monitoring program. It consisted of acquiring, processing, and interpreting 2D and 3D surface seismic and 2D vertical seismic profile (2D VSP) data sets (Figure 3) (Alshuhail et al., 2011). The main objective of the seismic program is to verify the CO_2 plume, and to evaluate the integrity of the storage (Alshuhail et al., 2011).

A baseline program (or phase I) of 2D surface seismic, acquired in March 2005, consists of two, multi-component, parallel lines, 400 m apart and oriented east-west. A third orthogonal line is oriented north-south intersecting the other two lines near the CO_2 injector well (Figure 3) (Lawton et al., 2005). Each line is a 3 km long with 20 m receiver interval, 40 m source spacing, a 2 kg dynamite charge at 15 m depth, approximately 3000 m maximum source-receiver offset, and a record length of 4 seconds with a sample rate

of 1 ms. In addition, the observation well had eight triaxial geophones cemented at 20 m intervals at depths between 1470 m and 1640 m with the deepest geophone within the Cardium reservoir.

Phase II of the seismic data set was acquired in December 2005, with similar geometry as phase I, and after injecting approximately $15,000$ tonnes of CO_2 in the reservoir. Phase III seismic program was acquired in March 2007 with similar geometry as the previous two phases, but with the addition of a $3km$ long 2D line (Line 6) trending southwest-northeast and a high resolution 16-level vertical seismic profiling (recorded in the western injector well). Table 2 summarizes the time-lapse seismic program at the CO_2-EOR study site.

Table 2: Summary of the seismic program at the CO_2-EOR study site (Alshuhail et al., 2011).

Phase	Seismic Data	Date	Injected CO_2 (tonnes)
I (baseline)	i. Line 1 (north-south) ii. Lines 2 and 3 (east-west) iii. Fixed-array VSP (8 geophones)	March 2005	0
II (1^{st} monitor)	i. Line 1 (north-south) ii. Lines 2 and 3 (east-west) iii. Fixed-array VSP (8 geophones)	December 2005	$15,000$
III (2^{nd} monitor)	i. Line 1 (north-south) ii. Lines 2 and 3 (east-west) iii. Fixed-array VSP (8 geophones) vi. Addition of - (a) 16-level VSP (b)southwest-northeast 2D line (line 6).	March 2007	$60,000$

The acquired seismic data sets were processed using the standard processing flow-through to post-stack time migration. Table 3 summarizes the processing flow that have been highlighted in several CREWES reports such as Lu et al. (2006).

Table 3: The standard processing work flow of the surface seismic data set (Lu et al., 2006).

Processing work flow for the PP data
Geometry assignment
Ground roll attenuation
Trace edits
Amplitude recovery
Minimum phase deconvolution
Tomographic structure statics
Velocity analysis
Surface-consistent residual statics
Spectral whitening
Mute and trim statics
Surface-consistent scaling
CDP stack
F-X noise attenuation
Poststack kirchhoff migration
Bandpass filter

Well 102/07-11-048-09 penetrated the Cardium and the Blackstone Formations. The computed synthetic seismograms (from the acquired dipole sonic log and calculated density) matched the surface seismic data quite well (Figure 4). The top of the Ardley Coal

Zone is a strong peak picked at a depth of 440 m at the well location which corresponds to 360 ms on the PP data. The next event is the top of the Cardium Formation which correlates to a weak peak at approximately 1043 ms in the PP data (about 1610 m TVD) and the top of the Blackstone Formation correlates to a weak trough at about 1060 ms in the PP data (about 1635 m TVD).

Figure 5 shows processed PP data of Line 1 from Phase I and III only since these surveys were recorded at the begining and the end of the monitoring project and are expected to have the largest time-lapse differences. The data quality is excellent and main reflections were easy to pick starting from the shallow top Ardley Coal Zone to the Viking Formation which is sandstone dominated zone. The Cardium Formation is a low impedance unit on the baseline seismic, and even after injecting the CO_2 gas, it shows as a low amplitude on the monitor survey. The difference section (Figure 5) after applying a poststack matching filter above the reservoir shows no clear anomalies at or below the Cardium Formation. At the top of the Ardley, a small amplitude residual is seen on the difference section and is attributed to low amplitude residual migration noise (Alshuhail et al., 2011).

The time-lapse processed PP VSP section for Line 1 is shown in Figure 6. As expected, the VSP data show higher bandwidth than the surface seismic data, particularly if we examine the Cardium event amplitude response which is stronger in the VSP data compare to the surface seismic data. On the difference section, there is an observed amplitude anomalies and time differences at the Cardium reservoir even though the VSP data is limited to about 100 m at the top of the reservoir due to geophone array depth and limited vertical aperture.

THE SURFACE-CONSISTENT MATCHING FILTERS

In previous reports and publications (Almutlaq and Margrave, 2010, 2012a), we showed that the surface-consistent data model can be extended to the case of designing matching filters to equalize two seismic surveys. Any trace in a baseline seismic survey may be modeled as follows:

$$d_1(t) \approx s_1(t) * r_1(t) * h_1(t) * y_1(t), \tag{1}$$

where subscript 1 refers to the baseline survey. Similarly, the corresponding trace from a monitor seismic survey (with subscript 2) may be modeled as

$$d_2(t) \approx s_2(t) * r_2(t) * h_2(t) * y_2(t). \tag{2}$$

Here we assume that the two surveys have exactly the same geometry. Fourier transforming equations 1 and 2, forming their ratio, and linearizing by taking the logarithm of both sides, we obtain

$$\log\left(\frac{\widehat{d_1}(\omega)}{\widehat{d_2}(\omega)}\right) \approx \log\left(\frac{\widehat{s_1}(\omega)}{\widehat{s_2}(\omega)}\right) + \log\left(\frac{\widehat{r_1}(\omega)}{\widehat{r_2}(\omega)}\right) + \log\left(\frac{\widehat{h_1}(\omega)}{\widehat{h_2}(\omega)}\right) + \log\left(\frac{\widehat{y_1}(\omega)}{\widehat{y_2}(\omega)}\right), \tag{3}$$

where ω is frequency, the "$\widehat{\ }$" denotes the Fourier transform. The left-hand side of equation 3 is the data log spectral ratio and the right-hand side contains the sum of surface-consistent terms. Using equation 3 to form a linear system of equations, we can create a separate linear system for each frequency, where each such system has one equation per trace.

This spectral ratio of the data term is a matching filter (Almutlaq and Margrave, 2012a) that can be decomposed into four-terms: source, receiver, offset and midpoint. We noticed that solving for the matching filters by spectral ratio, theoretically provide an exact solution, however it is difficult to obtain due to stability issues when dealing with seismic data because of noise. Alternatively, solving the time-domain least squares matching filters then Fourier transforming the result is a stable approximation to the spectral ratio.

APPLICATION TO FIELD DATA AND ANALYSIS

We choose a 2D time-lapse seismic line from the Violet Grove as a pilot test for the surface-consistent matching filters. Line 1 (Figure 3) is a north-south which passes through the west CO_2 injector well. We are only investigating the repeated PP shots in both the baseline and the monitor. The method of computing the matching filters is a topic discussed in details in another report in this volume (Almutlaq and Margrave, 2012b), and in this report we only discuss the application to field data as well as the interpretation.

There are 66 repeated shots for this line. After we assign the geometry, we attenuate coherent noise, such as ground rolls. The monitoring survey contains more noise compared to the baseline and even after attenuating most of the coherent noise in the pre-processing stage, some noise level is still observed in the monitor data (Figure 7). Table 4 summarizes the processing steps for Line 1.

Table 4: Processing work flow of Line 1.

Baseline	**Monitor**
Geometry assignment	Geometry assignment
Ground roll attenuation	Ground roll attenuation
Trace edits	Trace edits
Amplitude recovery	Amplitude recovery
Surface consistent Amplitudes correction	Surface consistent Amplitudes correction
Surface consistent Spiking deconvolution	Surface consistent Spiking deconvolution
-	**Surface consistent matching filters**
Velocity analysis	-
Surface-consistent residual statics	Surface-consistent residual statics
CDP stack	CDP stack

We compute and apply the four-components surface-consistent matching filters for a shallow window above the reservoir as highlighted in Figure 7. The window is centered on the Ardley Coal which is a relatively good reflector on shot gathers. The difference between the baseline survey and the monitor survey is quite large at this level. After applying the matching filters the difference reduced slightly (Figure 7) but due to the high level of noise in the shallow section, the overall result is not satisfactory.

We select a deeper window below the reservoir to examine the algorithm. Ideally only intervals above the reservoir should be matched, however in this case we do not have good reflectors above the reservoir other than the Ardley Coal. Figure 8 shows a shot record from the middle of Line 1 (we are only showing the right half of the shot record). The difference is large caused by a combination of amplitude and time. After computing and applying the four-terms surface-consistent matching filters to the monitor data set, observed amplitude and time differences are reduced (Figure 9. The matching is not perfect and

possibly requires a second iteration. We also notice that the noise dominates the near offset traces and if that is separated from the far offset ones, we might improve the result. Figure 10 illustrates another example of a shot record closed to the south end of the line. Note the large amplitude difference between the monitor and the baseline. After matching (Figure 11), the amplitude difference is less apparent and the difference is smaller.

Figure 12 illustrates the stack difference of the baseline and the monitor. The difference on the stacked data is still large. After applying the surface-consistent matching filters (Figure 13) , the difference reduced significantly. This result is encouraging and although it is not the end of this work, it illustrates the progressive decrease of the error after applying the surface-consistent matching filters. Matching filters should also be repeated to reduce remaining amplitude and time residuals. After that, velocity analysis and surface-consistent static correction should also be repeated to improve the result.

Comparing this result at this stage with previous processing is not informative since both are not at the same processing stage. Repeating the process for the window above the reservoir is required, particularly after all the learning from applying the matching filters to the deeper window. Velocity analysis, residual static correction should be repeated and finally migrate the data in order to prepare it for comparison with previous processing.

It is important to mention here that we are using previous processing result to benchmark the application of the surface-consistent matching filters. Reproducing similar result is considered a success for this method, particularly since we are aware that careful time-lapse processing was performed on the previous processing.

CONCLUSIONS

In summary, we successfully apply the surface-consistent matching filters to a real data set from Violet Grove area in central Alberta. The time-lapse difference due to CO_2 has not been investigated in this study even though previous reporting concluded that it was difficult to detect on surface seismic. Despite that, we decide to use one line from this data set to examine the matching filters algorithm. We evaluate two zones: a shallow one above the reservoir centered on the Ardley Coal Zone, and a deeper one below the reservoir. Generally, zones below reservoir are not matched, however, our data only has one good seismic reflector (Ardley reflector) above the reservoir, hence, the deeper zone is examined for testing algorithm only.

A large amplitude and time residual is observed in this data set. After computing and applying the surface-consistent matching filters to the shallow window, large differences remained. This is due to the high noise level due to its proximity to the near surface layer known for its low velocity and incoherent noise generation. However, in the deeper window we observe a some improvement to the result on both pre-stack and post-stack data. Some of the mismatch observed between the baseline survey and the monitor survey has been reduced after applying the matching filters. We expect that widening the window of the matching filter and iterating the process will improve the result. Other processes such as residual statics and migration will be applied to reduce remaining mismatches.

ACKNOWLEDGEMENTS

The authors thank the sponsors of CREWES for their continued support, CREWES staff and students. A special thank you to Helen Issac, Down Lawton, Kevin Hall, and David Henley for their help. Mahdi Almutlaq expresses his gratitude to Saudi Aramco for sponsoring his PhD program.

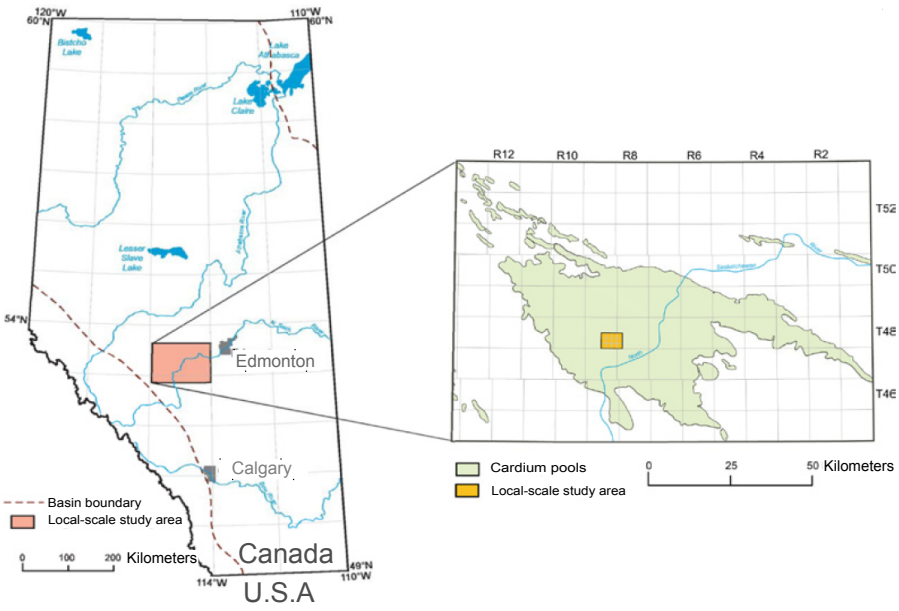

FIG. 1: Map of Alberta showng the location of the Pembina Oil Field and the CO_2-EOR pilot site at Violet Grove (Dashtgard et al., 2006).

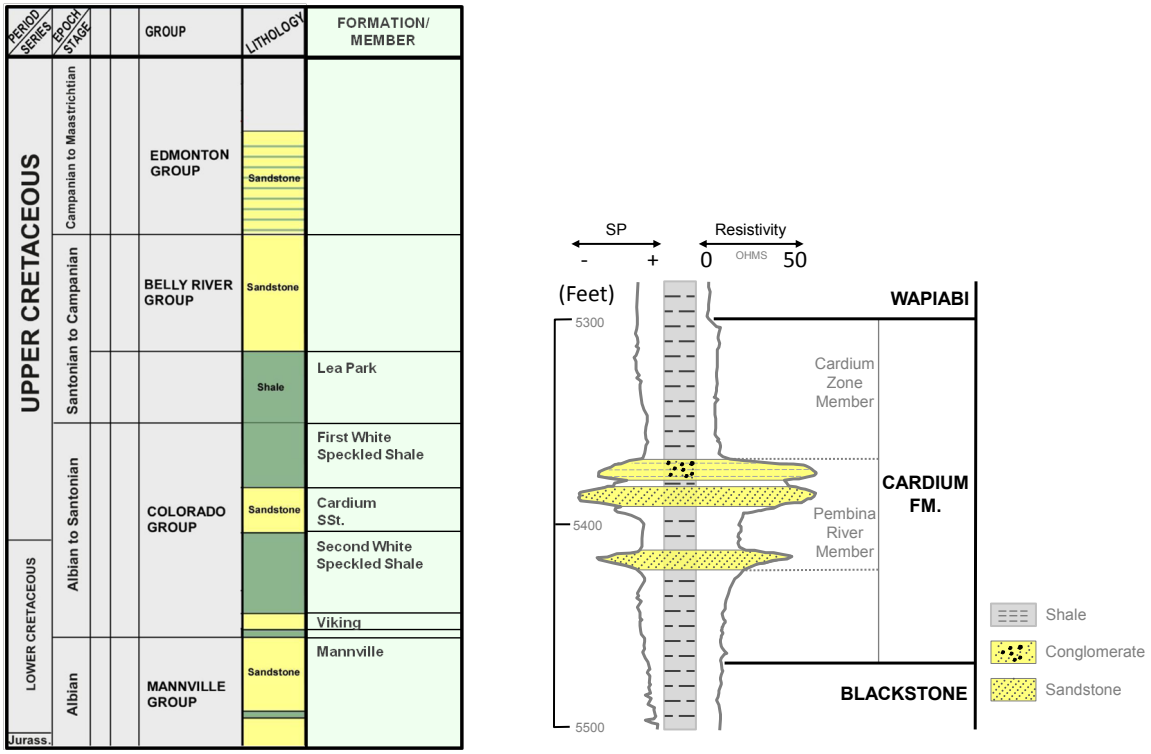

(a) (b)

FIG. 2: General stratigraphic column of central Alberta of the Lower and Upper Cretaceous (Bachu and Bennion, 2008) shown in (a) and a typical well log from the Pembina Field showing the Cardium Formation in (b); a modified plot of that in Patterson (1957).

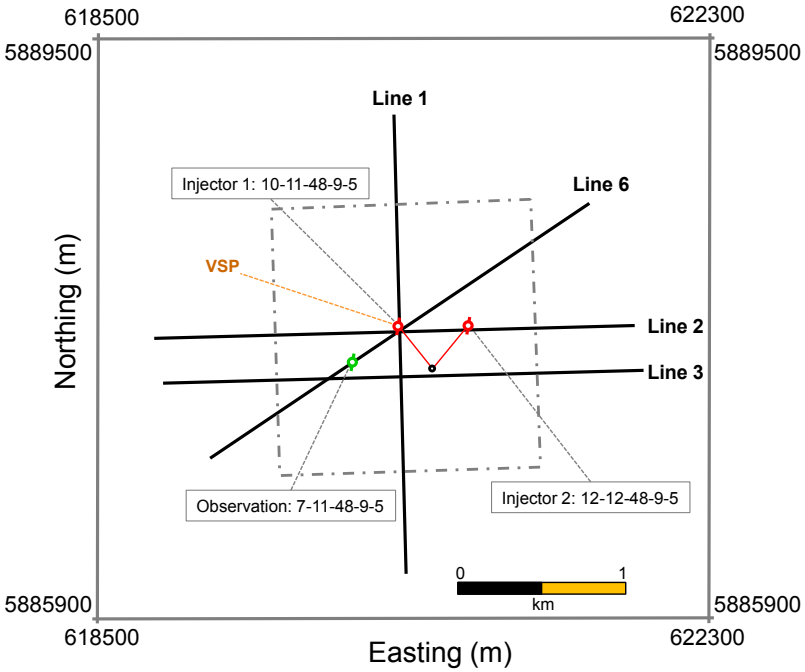

FIG. 3: Layout of the surface seismic lines, 3D seismic coverage (indicated by the dashed rectangle), and location of the injector wells, observation well, and VSP (Lawton et al., 2005).

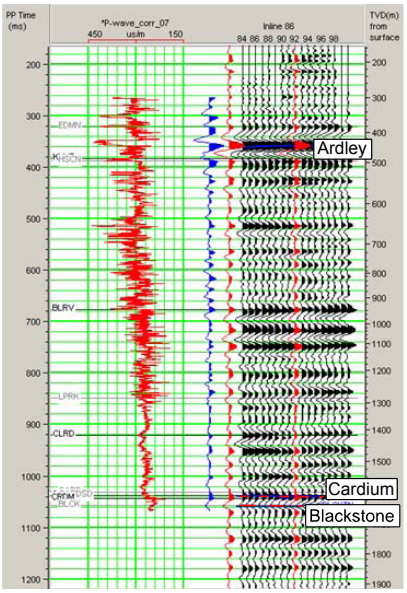

FIG. 4: PP seismic correlation at well $102/7-11-48-9$. The blue trace is synthetic seismogram, and the red trace is extracted from the surface seismic at the well location (Chen, 2006).

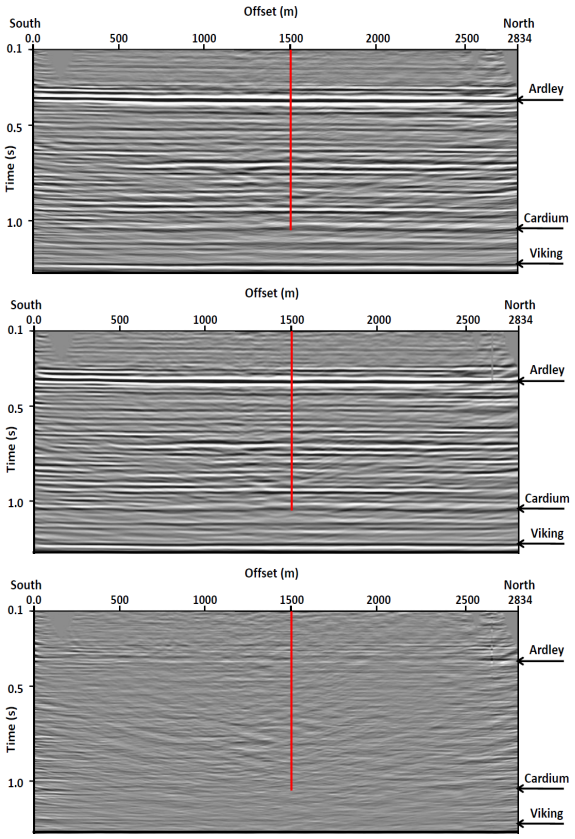

FIG. 5: Processed PP data from Line1 (Alshuhail et al., 2011). Top is Phase I (baseline), middle is Phase III (monitor), and bottom is difference after applying post stack matching filter to the interval above the Cardium reservoir. The red line is the projection of the $102/7-11-48-9$ well.

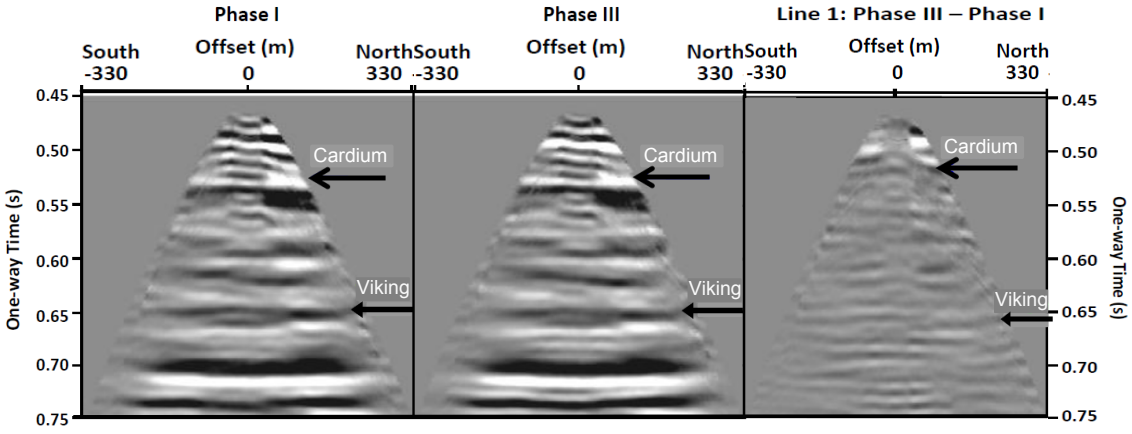

FIG. 6: Walkaway PP VSP data from Line1 at the observation well (Alshuhail et al., 2011). On the left is Phase I , middle is Phase III, and on the right is the difference.

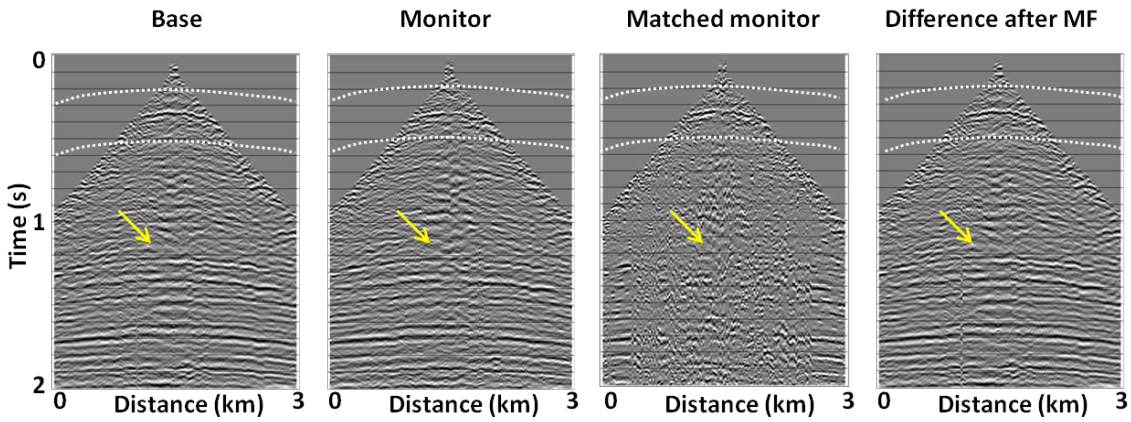

FIG. 7: A shot record from the baseline survey, same shot from the monitor survey, matched monitor shot, and finally the difference between the baseline shot and the matched monitor shot. The dashed white lines illustrate the window of interest. The yellow arrow is the reservoir.

REFERENCES

Almutlaq, M. H. and Margrave, G. F. (2010). Towards a surface-consistent match filter (SCMF) for time-lapse processing. *CREWES report*, (22):1–17.

Almutlaq, M. H. and Margrave, G. F. (2012a). Surface-consistent matching filters for time-lapse processing. *SEG Expanded Abst.*

Almutlaq, M. H. and Margrave, G. F. (2012b). Surface-consistent matching filters for time-lapse seismic processing. *CREWES report*, (24):1–22.

Alshuhail, A. A., Lawton, D. C., and Chabot, L. (2011). Pembina cardium CO_2 monitoring project: time-lapse seismic analysis. *CREWES report*, (20):1–18.

Arts, R., Eiken, O., Chadwick, A., Zweigel, P., Meer, L., and Zinszner, B. (2002). Results and experiences from the first industrial-scale underground CO_2 sequestration case (Sleipner Field, North Sea). *IEA 6th international conference*.

Avseth, P., Mukerji, T., and Mavko, G. (2005). *Quantitative seismic interpretation: applying rock physics tools to reduce interpretation risk (1st ed.)*. Cambridge University Press.

Bachu, S. and Bennion, B. (2008). Effects of the in-situ conditions on relative permeability characteristics of CO_2-brine system. *Environ Geol*, (54):1707–1722.

Brown, L., Davis, T., and Batzle, M. (2002). Integration of rock physics, reservoir simulation, and time-lapse seismic data for reservoir characterization at Weyburn Field, Saskatchewan. *SEG Exp. Abst.*

Chadwick, A., Noya, D., Artsb, R., and Eikenc, O. (2009). Latest time-lapse seismic data from Sleipner yeild new insights into CO_2 plume development. *Energy Procedia*.

Chen, F. (2006). Interpretation of time-lapse surface seismic data at a CO_2 injection site, violet grove, alberta. *MSc. Thesis, University of Calgary*.

Dashtgard, S., Buschkuehle, M., Berhane, M., and Fairgrieve, B. (2006). Local-scale baseline geological report for the Pembina-Cardium CO_2-enhanced oil recovery site. *Alberta Geological Survey*, (Alberta Energy and Utilities Board).

Davis, T., Terrell, M., C. R., and Winarsky, W. (2003). Multicomponent seismic characterization and monitoring of the CO_2 flood at Weyburn Field, Saskatchewan. *TLE*, (22).

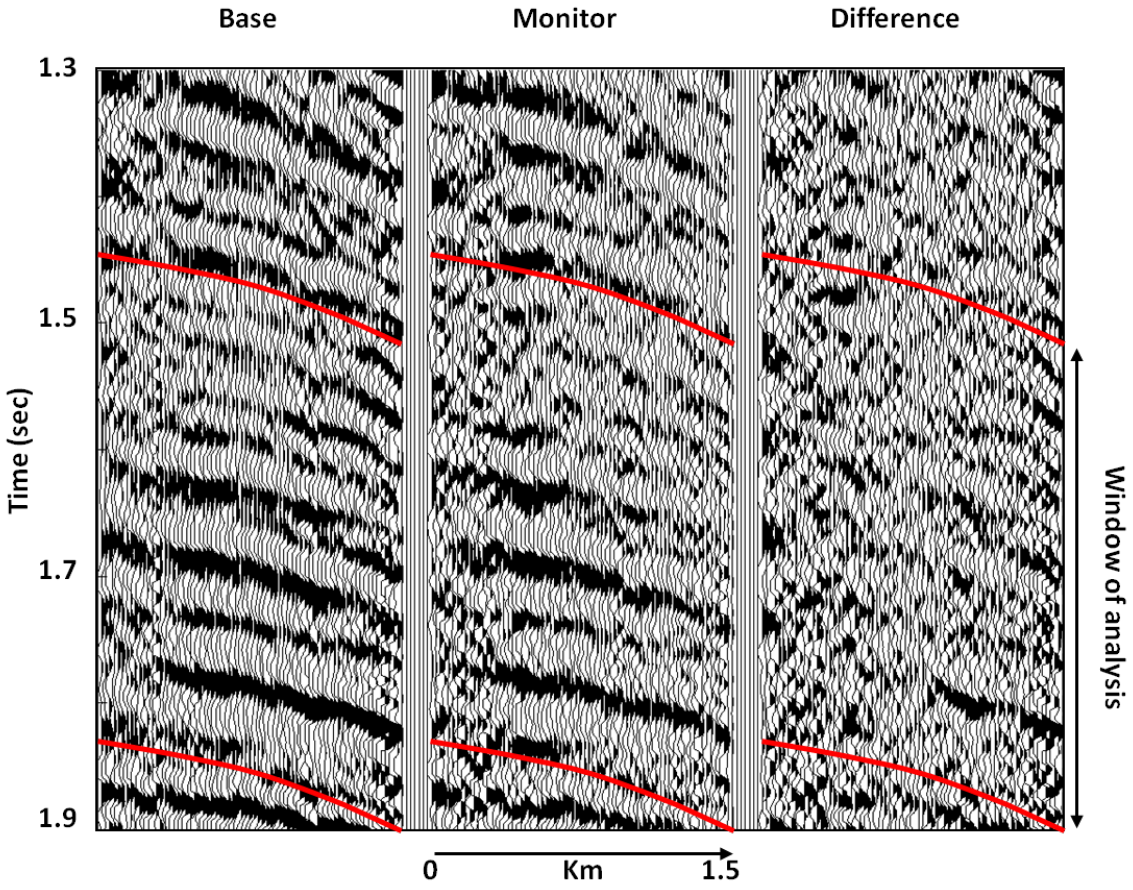

FIG. 8: Same shot record as that shown in Figure 7, except in here we show the section below the reservoir and only the right half of the shot. Note the large difference in the window of analysis.

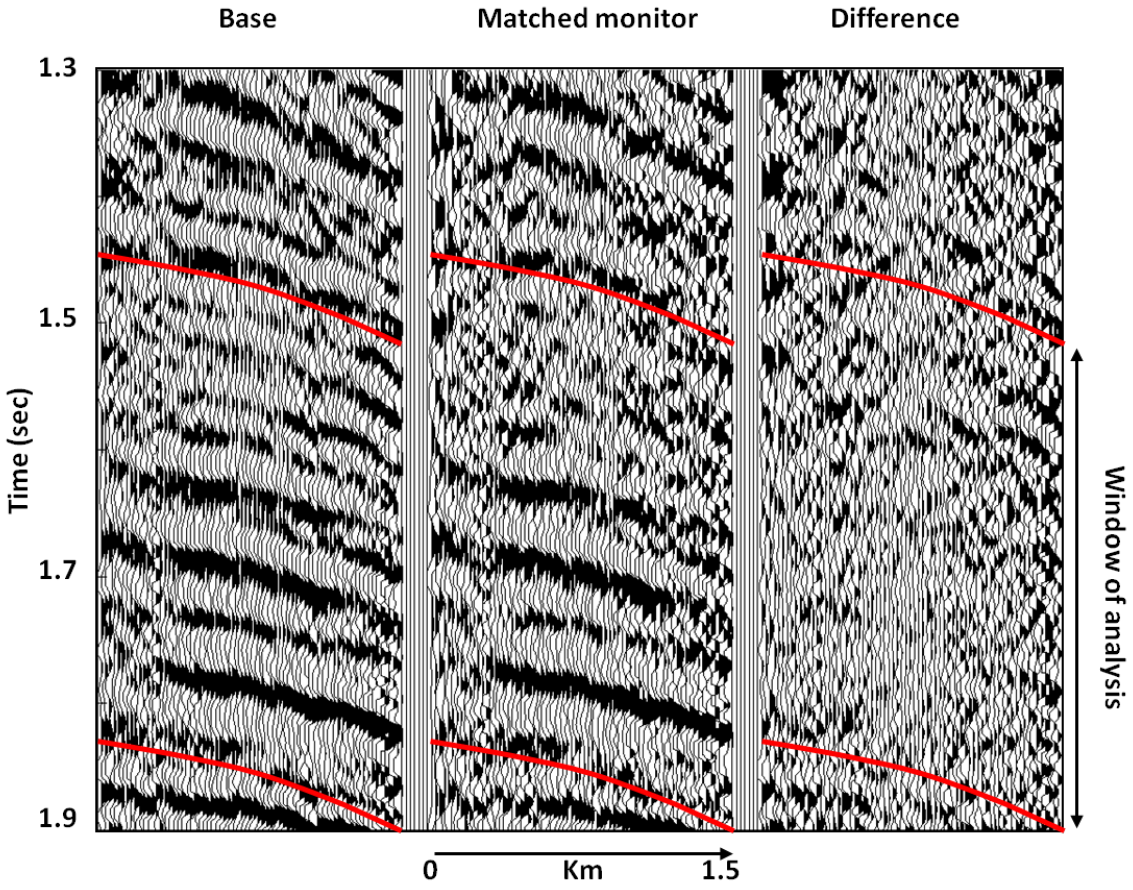

FIG. 9: Baseline shot (left), monitor shot after applying the matching filters (middle), and the difference (right). Note the difference has decreased significantly in the window of analysis.

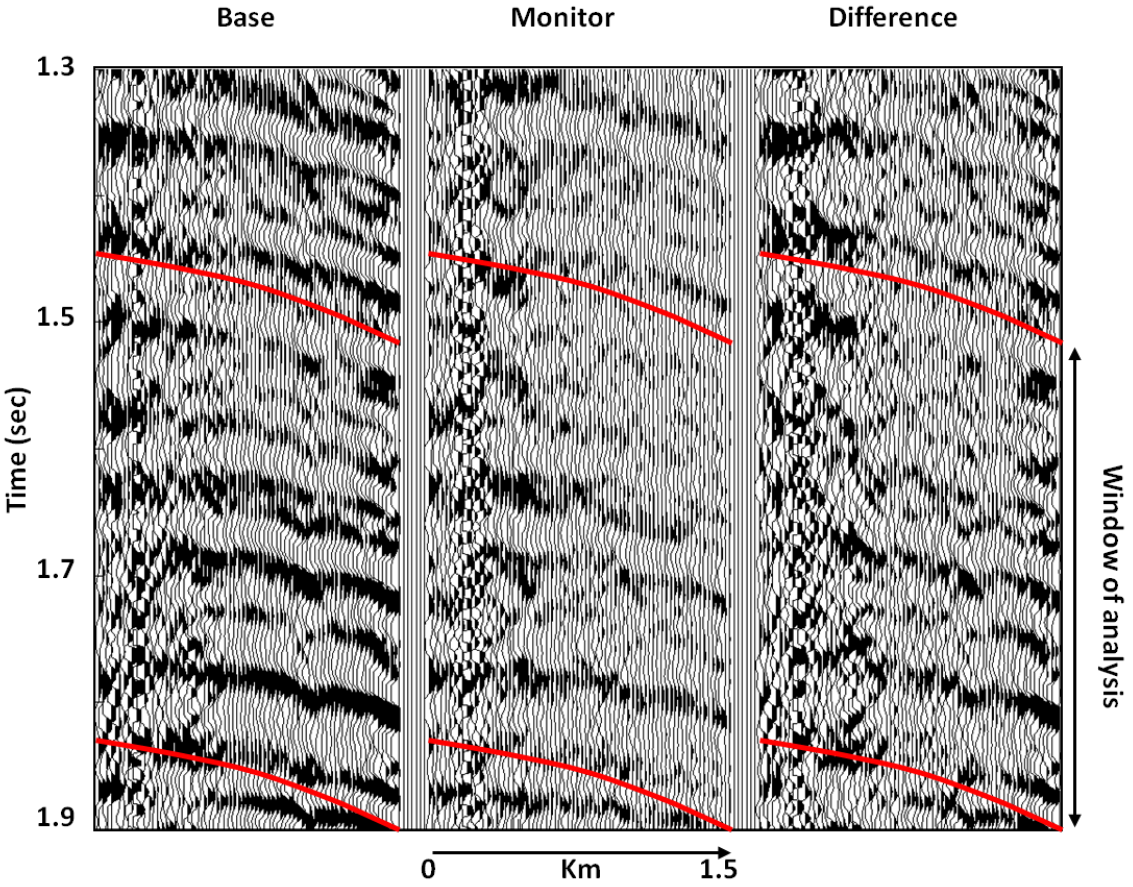

FIG. 10: Another example of baseline and monitor shots 200 m away from previous example. Note the large difference and the high noise level on the near offset traces.

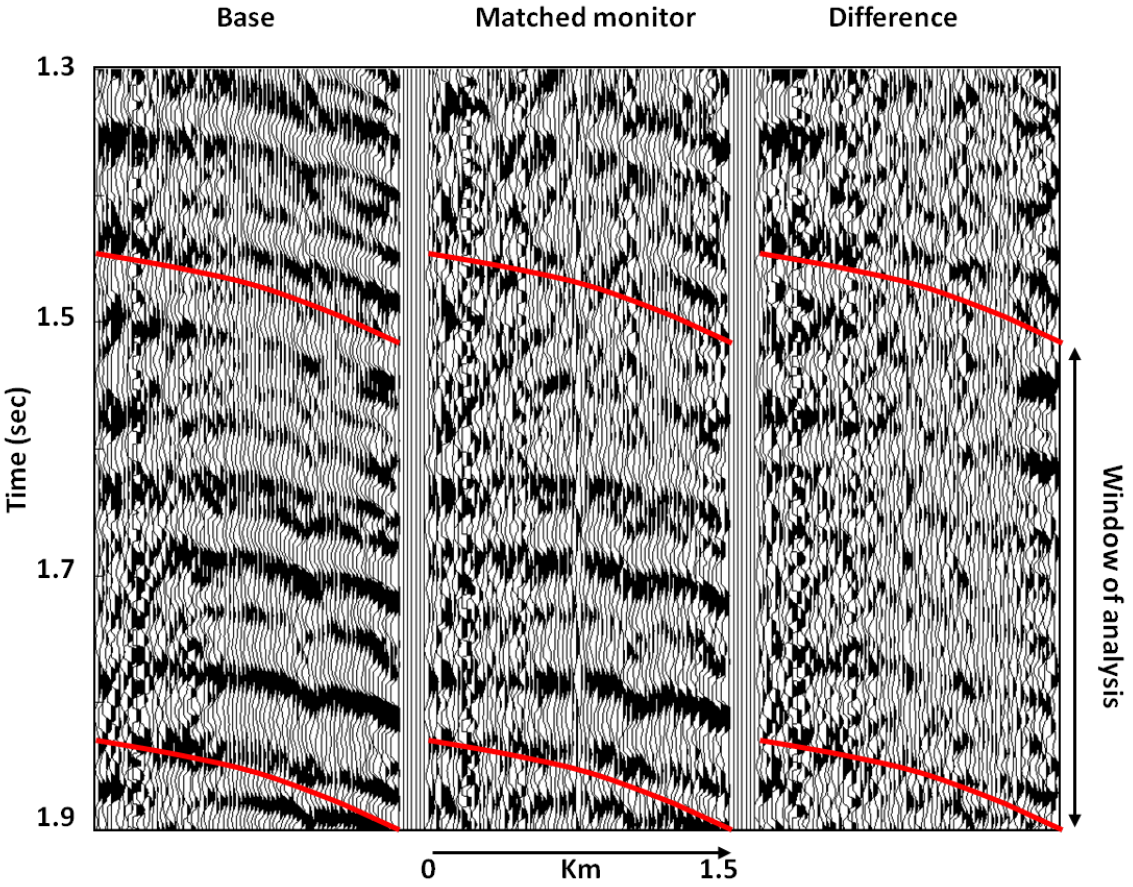

FIG. 11: The same shot shown in Figure 10 (left), the matched monitor (middle), and their difference (right). Note the decrease in mismatch except where noise is high.

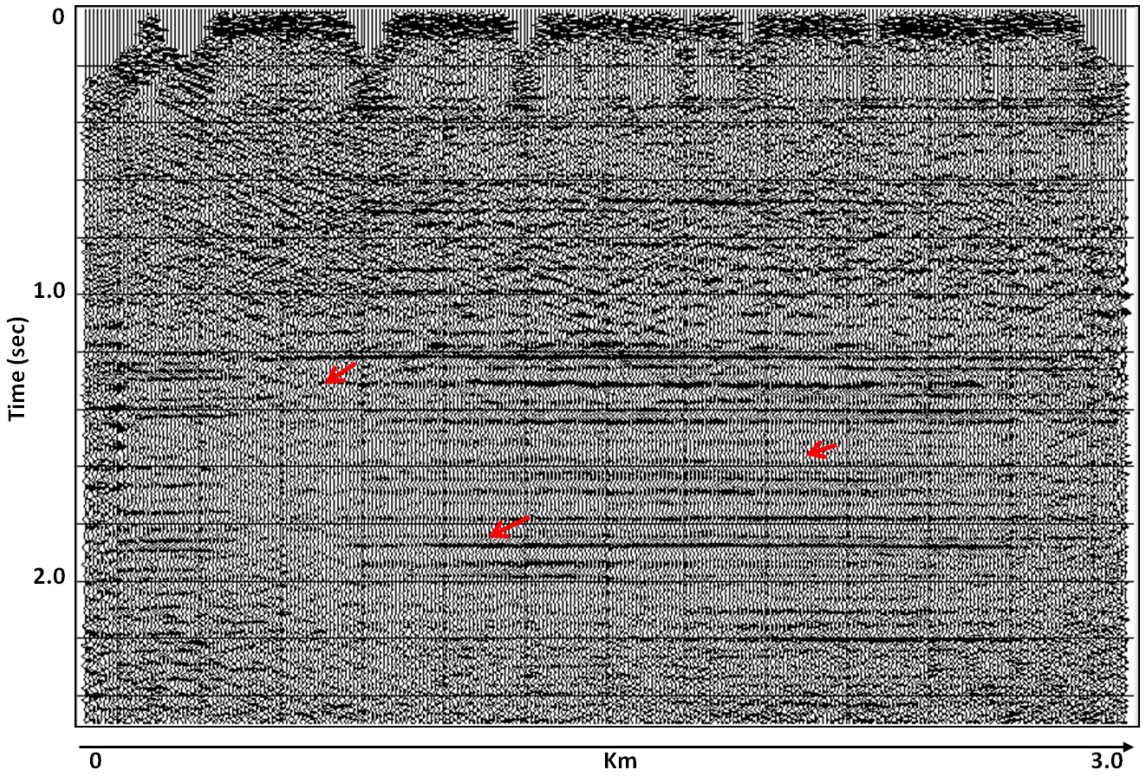

FIG. 12: Stack difference between baseline and monitor before matching filters.

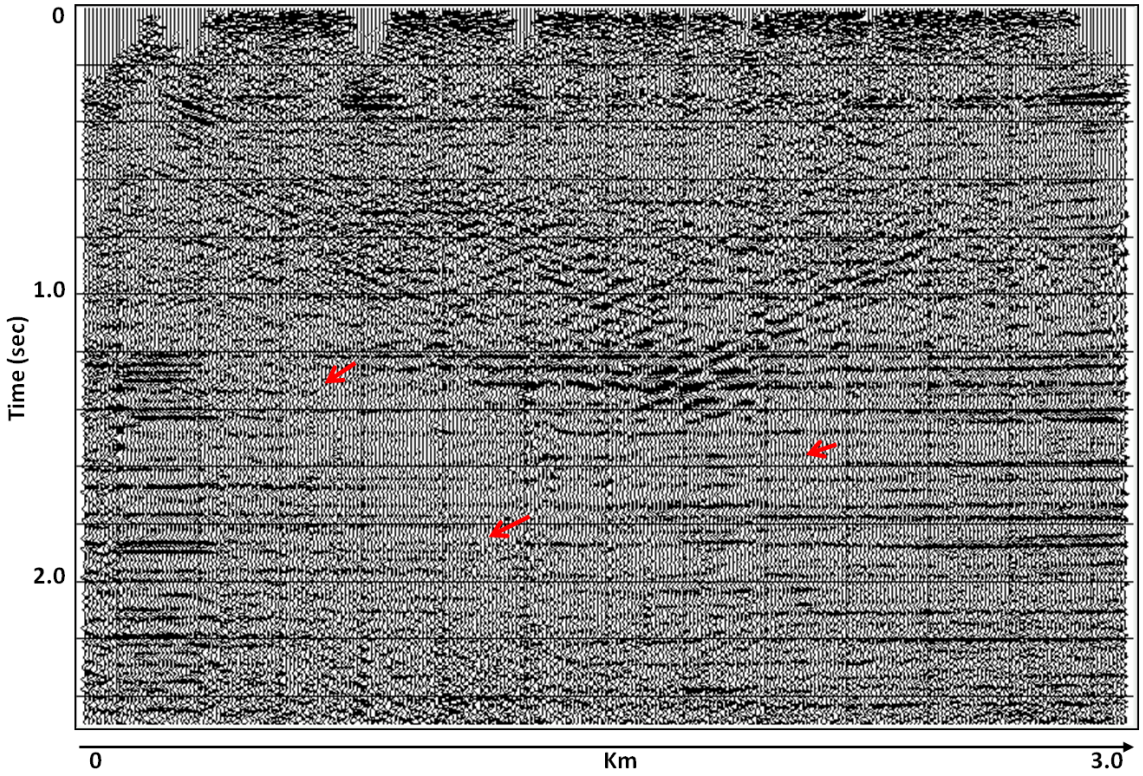

FIG. 13: Stack difference between baseline and monitor after matching filters.

Hilterman, F. (2001). Seismic amplitude interpretation. *SEG/EAGE Disc.*

Hitchon, B. (2009). *Pembina Cardium CO_2 monitoring pilot: A CO_2-EOR project, Alberta, Canada*. Geoscience publishing.

Lawton, D., Coueslan, M., Chen, F., Bland, H., Jones, M., Gallant, E., and Bertram, M. (2005). Overview of the Violet Grove CO_2 seismic monitoring project. *CREWES report*, (17):1–24.

Li, G. (2003). 4D seismic monitoring of CO_2 flood in a thin fractured carbonate reservoir. *TLE*, (22).

Lu, H., Hall, K., and Lawton, D. (2006). Violet grove 2D data processing at CREWES update. *CREWES report*, (18):1–17.

MacBeth, C. and Lynn, H. (2000). Fracture-related reflectivity in applied seismic anisotropy: Theory, background, and field studies. *SEG Geophysics reprint series No. 20*.

Mavko, G. and Mukerji, T. (1998). Bounds on low-frequency seismic velocities in partially saturated rocks. *Geophysics*, (63):918–924.

Patterson, N. R. (1957). Geology of the Pembina field, Alberta. *Bulletin of the AAPG*, (41):937–949.

Terrell, M., Davis, T., Brown, M., and Fuck, R. (2002). Seismic monitoring of a CO_2 flood at Weyburn Field, Saskatchewan, Canada: demonestrating the robustness of time-lapse seismology. *SEG Exp. Abst.*

Wang, Z. (2001). Fundamentals of rock physics. *Geophysics*, (66):398–412.

Wang, Z., Cates, M., and Langan, R. (1998). Seismic monitoring of a CO_2 flood in a carbonate reservoir: A rock physics study. *Geophysics*, (63):1604–1617.

White, D. (2009). Monitoring CO_2 storage during EOR at the Weyburn-Midale Field. *TLE*, (28).

Zweigel, P., Arts, R., Bidstrup, T., Chadwick, A., and Gregersen, U. (2001). Results and experiences from the first industrial-scale underground CO_2 sequestration case (Sleipner Field, North Sea). *AAPG Exp. Abst.*